## PAPER

# Soft-lithographic patterning of room temperature-sintering Ag nanoparticles on foil†

Pieter F. Moonen,[a] Erhan Bat,[a] W. Pim Voorthuijzen[b] and Jurriaan Huskens*[a]

Room temperature-sintering, poly(acrylic acid)-capped silver nanoparticles (Ag-PAA NPs) were used in a wide range of nanofabrication methods to form metallic silver microstructures on flexible poly(ethylene terephthalate) (PET) substrates. Silver wires on top of PET foil were patterned by micromolding in capillaries (MIMIC), and silver wires embedded in SU8 on PET foil were fabricated by wetting-controlled deposition in open microchannels. One hundred μm-wide Ag microwires with lengths of 5–15 mm, heights of 0.6–2.5 μm, and a maximum conductivity of a factor 7.3 lower than bulk Ag were obtained. Methanol was studied as an alternative dispersing solvent. It sped up MIMIC drastically, but the low particle packing quality and pre-coalescence in solution resulted in a higher resistivity. The sintering depth was found to be limited to around 100 nm for HCl-vapor induced sintering. Aqueous NaCl, added in a concentration below 50 mM to the Ag-PAA NP ink, was investigated as self-sintering agent. It resulted mainly in strong particle clustering and formation of numerous non-connected grains upon the evaporation of water. A hydrogel reservoir stamping system was used as an alternative printing technique for the transfer of the Ag-PAA NP ink on a PDMS substrate to yield the repetitive printing of arrays of 144 three-micron-wide Ag dots.

## Introduction

The fabrication of metallic, conductive structures in plastic electronics is an emerging field of research. A market with annual revenues estimated at more than 200 billion Euro is foreseen in the near future by combining a highly viable and innovative fusion of three technological areas: microelectronics, chemistry and printing.[1] The smart use of metallic inks to render patterned structures conducting when deposited at polymer substrate-friendly temperatures (<150 °C),[2] enables thin, flexible, light-weight and low-cost electronic devices. Potential applications are organic photovoltaics,[3,4] transistors,[5] and radio frequency identification (RFID) tags.[6–8]

Metallic inks are often composed of precursor materials, including metallic nanoparticles (NPs) and metal–organic decomposition (MOD) inks. NP inks are formed by dispersing the NPs in aqueous or organic solvents and often adding colloidal stabilizers. Uniform and monodisperse NPs contribute thereby to a high colloidal stability and low electrical resistivity at low metallization temperatures.[9,10] MOD inks, such as a Ag salt dissolved in a suitable solvent,[11] form NPs *in*

*situ* upon destabilization during a solution step. NP inks usually have a higher metal loading[1,16] compared to MOD inks and are more widely available commercially. Metal structures made from NP inks generally exhibit a higher conductivity and contact resistances have been reported to be 5–10 times lower.[12] On the other hand, MOD inks do not require colloidal stabilizers and reduce nozzle clogging when used in inkjet printing, an often reported patterning technique for both inks.[9,10,13,14] Writing a Ag NP ink with a rollerball pen on paper with a resolution down to 250 μm is probably the most simple and broadly accessible patterning technique reported in literature.[7]

Both types of ink require an additional sintering or decomposition step to render the precursor material conductive. Typically, heat is used to precipitate the metal and to burn off the organic ligand in MOD inks, or, in the case of NP inks, to decompose the organic stabilizer. The organic stabilizing agent introduces a balance between the dispersion stability, printability of the ink and the sintering temperature.[1,16] The sintering temperature, defined as the temperature at which all organic material has been burnt off and necks begin to form between the particles, depends for metal NP inks on the size of the nanoparticles.[1] Sintering typically requires >30 min process time and/or higher temperatures (>250 °C) to form continuous, albeit percolating network, metal structures.[1] However, high sintering temperatures are incompatible with common low-cost polymer foils, such as poly(ethylene terephthalate) (PET) and polycarbonate (PC),

[a]*Molecular Nanofabrication Group, University of Twente, P.O.Box 217, 7500 AE, Enschede, The Netherlands. E-mail: J.Huskens@utwente.nl; Fax: +31 (0)53 4894645; Tel: +31 (0)53 489 2995*

[b]*Holst Centre/TNO, High Tech Campus 31, 5656 AE, Eindhoven, The Netherlands*
† Electronic supplementary information (ESI) available: Additional optical microscopy images and cross-sectional profiles to determine the resistivity are shown. See DOI: 10.1039/c3ra43926g

that have a relatively low glass transition temperature. The choice of foil is therefore restricted to more expensive polymers such as polyimide (PI),[1] or the sintering temperature has to be drastically reduced. Lower sintering temperatures have been obtained by formulating a Ag ink with a low content of organic stabilizers. It revealed a conductivity of 5–65% of bulk Ag at a sintering temperature of 80 °C, but the low content of binding materials complicated the use in inkjet printing.[14] Recently, an MOD ink was reported resulting in bulk conductivity of Ag after 15 min sintering at 90 °C.[11] Although a very good conductivity was obtained in this study, the long sintering time makes it unsuited for high-throughput patterning in, for example, a roll-to-roll line.

Magdassi et al.[9,15] reported a room temperature-sintering NP ink composed of Ag–poly(acrylic acid) (Ag–PAA) NPs. This ink is destabilized by exchange of PAA for a halide, inducing not only the destabilization of the ink by detaching the PAA anchoring groups but also the coalescence of the Ag NPs, hereby dramatically increasing the conductivity to approximately 10% of bulk Ag while the particle size increases from ∼15 nm single particles to agglomerates of 0.2–6 μm. The ink destabilizes and sinters in solution above a critical Cl⁻ concentration of 50 mM. Addition of NaCl in a concentration below 50 mM to the aqueous dispersion of Ag–PAA NP ink resulted in room-temperature sintering upon solvent evaporation. A conductivity of up to 41% of that of bulk Ag was obtained by post-sintering inkjet-printed and dried Ag–PAA NPs by a short (10 s) exposure to HCl vapor. Perelaer et al.[16] obtained 60% bulk silver conductivity by Ar plasma pre-sintering for 8 min and microwave flash sintering for 1 s at 1 W for 5 mm long lines. Smaller or larger line lengths showed a conductivity of 20% of bulk Ag.

Here we describe the compatibility of the fast and room temperature-sintering Ag–PAA NP ink with three, low-cost patterning strategies on PET foil with the potential for large-area fabrication (Scheme 1). Therefore, conductive Ag microwires were patterned on PET foil by micromolding in capillaries (MIMIC), and Ag microwires were embedded in a resist mask on PET foil by wetting-controlled deposition. Arrays of few-micron sized Ag dots were deposited on an elastomeric substrate by the third patterning strategy, employing a hydrogel-based stamping device. Both the dimensions of the structures and their conductivity after sintering were assessed. Furthermore, a more rapidly evaporating solvent for the Ag-PAA NP dispersion was evaluated, and the effect of the layer thickness on sintering and the corresponding resistivity was studied.

## Results and discussion

Three patterning strategies were employed in this study (Scheme 1). In the first strategy (Scheme 1a), Ag microwires were formed on PET foil by patterning the Ag–PAA NP ink with MIMIC and subsequent sintering. The patterned, elastomeric mold for MIMIC was made by replica molding commercially
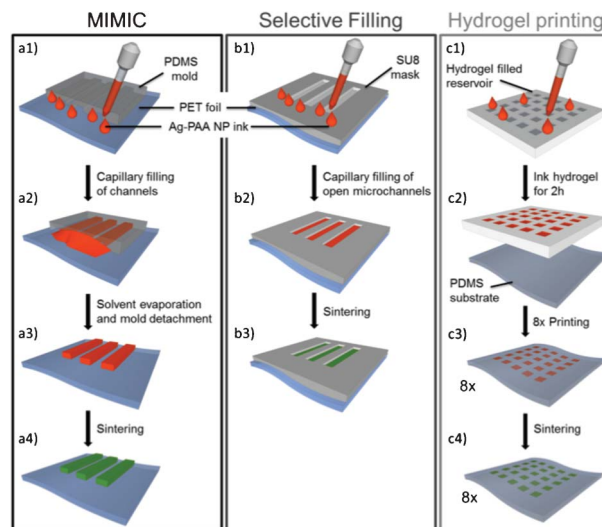


**Scheme 1** Representation of the three studied patterning techniques: (a) Ag microwires formed on top of PET by MIMIC; (b) Ag microwires embedded in an SU8 resist mask on PET foil; (c) few-micron-sized Ag dots printed from a hydrogel reservoir onto a PDMS substrate.

available poly(dimethylsiloxane) (PDMS) against a patterned Si wafer. Embedding of the Ag features in a chemically non-reactive and easily patternable mask is potentially more interesting in terms of a functional three-dimensional device. Embedded metal structures were obtained by the second patterning strategy (Scheme 1b), in which Ag microwires were formed in open microchannels in SU8 on PET foil.

An alternative patterning technique with the potential for high-resolution printing, typically not attainable with inkjet printing, was studied as well. Ag–PAA NPs were printed using a stamping device with hydrogel reservoirs to form arrays of Ag dots with a diameter of only a few microns (Scheme 1c).

### Ag wires on PET by MIMIC

Five millimeter long and 100 μm-wide, densely packed Ag-NP microwires were obtained over an area of 1 × 1 cm² on PET foil by MIMIC (Fig. 1a–b; see supplementary information† Fig. S1). Conformal contact between the PDMS mold and PET foil, activated by short exposure to O₂ plasma, formed closed channels (100 μm wide and spaced, 32 μm high) with two open ends on the PET foil. The channels were subsequently filled by placing a drop of Ag–PAA NP ink at one of the channel entrances (Scheme 1a1). The channels filled instantly upon capillary action (Scheme 1a2). The solvent was evaporated under a stream of N₂ within approx. 1 h, whereafter the elastomer mold was peeled off, leaving the patterned Ag wires on the foil (Scheme 1a3). Sintering was induced by destabilization of the patterned Ag-PAA NPs by exposure to HCl vapor for 5 min (Scheme 1a4).

Upon solvent evaporation, the Ag–PAA NP ink was dragged from the edges of the channel to the center (see Fig. S2, ESI†), leaving behind interrupted and thus non-conducting Ag agglomerations near the channel openings (Fig. 1c–d). A higher solid content of the ink, a stronger chemical
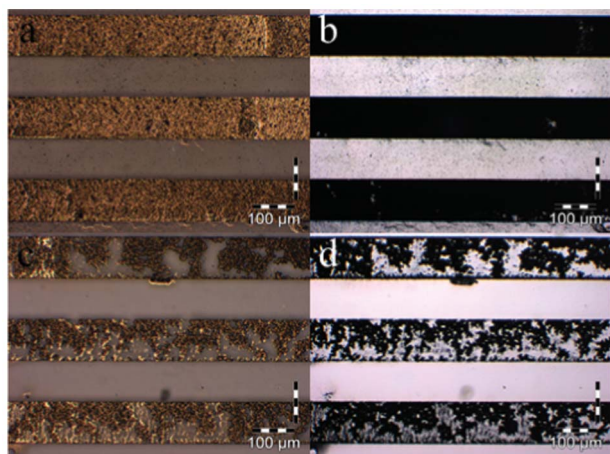
Fig. 1 Optical microscopy images in reflection (a, c) and transmission (b, d) mode in (a, b) the center of the MIMIC-patterned lines and (c, d) near the edges of the channels before sintering.

functionalization of the exposed substrate surface, and/or a drying stream leading from the center outwards to the channel openings might decrease the interrupted zone near the channel openings.

The electrical resistivity $\rho$ (in $\Omega m$) of the sintered Ag microwires was determined according to $\rho = R \times A/l$ (equation 1), with $R$ (in $\Omega$) being the electrical resistance, $A$ (in $m^2$) the cross-sectional area of the wire and $l$ (in m) the wire length.

The wire resistance $R$ over length $l$ was calculated by measuring the current $I$ (in A) as a function of the applied voltage $V$ (in V) in a two-point probe measurement. Three height profiles on different points along the Ag wire were measured with profilometry and averaged, whereafter the area underneath the curve was integrated to obtain an averaged value for $A$ (Fig. 2). The length of the wire was measured by optical microscopy.
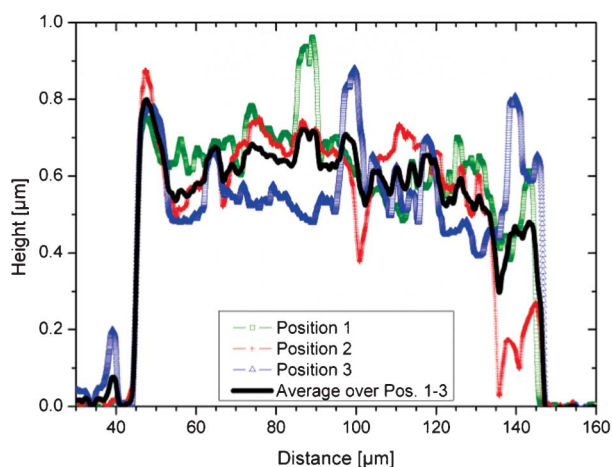


Fig. 2 Cross-sectional profiles and their average at several points of a Ag wire made by MIMIC and subsequent sintering.

From a measured resistance of 1.18 $\Omega$ over a wire length of 399 $\mu m$ with a cross-sectional area of 60.4 $\pm$ 2.3 $\mu m^2$, a resistivity of 43 $\pm$ 19 $\mu\Omega cm$ (average over three different wires) with a minimum of 17.9 $\mu\Omega cm$ was obtained for MIMIC-patterned, sintered Ag microwires on PET foil from aqueous Ag–PAA NPs. The larger deviation between the average and the best obtained resistivity likely originates from a deviation in the layer thickness over the length of the three measured wires. The obtained resistivity is, with a minimal value of 17.9 $\mu\Omega cm$, roughly a factor 11 higher than the resistivity of bulk silver ($\rho_{bulk} = 1.59$ $\mu\Omega cm$[17]). Although a factor 11 is already a good value for room temperature-sintered Ag NPs, Grouchko et al.[15] have reported a resistivity as low as 3.84 $\mu\Omega cm$ (factor 2.4) for Ag structures, deposited by inkjet printing, upon sintering in HCl vapor. Furthermore, a resistivity of 16 $\pm$ 2 $\mu\Omega cm$ was reported for Ag wires (width 95 $\mu m$, thickness 500 nm) formed by inkjet printing of a self-sintering silver dispersion with low NaCl concentration ([NaCl] < 50 mM). In this system, the NaCl concentration increased to above the critical value of 50 mM simply by water evaporation, leading to particle destabilization and formation of a conducting silver network. The authors mentioned a low-density packing of the NPs as an explanation for the higher resistivity, as a result of the immediate coalescence of the NPs in the liquid thereby hindering any optimization of the packing. With HCl vapor as the sintering agent, the process of destabilization and packing of the particles is separated, allegedly leading to minimal distortion of the packing during sintering and a higher conductivity. According to this interpretation, non-optimal particle packing might be the reason for the higher resistivity obtained here. MIMIC might hinder an optimal particle packing in the channel, due to contact angle-dependent drag of the contact line at the channel sidewalls.

The self-sintering of the Ag–PAA NP ink with NaCl in a concentration below the critical value of 50 mM as reported by Grouchko et al.[15] was studied as well. Therefore, an aqueous Ag–PAA NP dispersion with 40 mM NaCl was patterned by MIMIC on PET as described before. Evaporation of the solvent (water) induced instant, room temperature sintering forming silvery-shining microwires. However, the sintering resulted in strong clustering of the particles, forming numerous non-connected grains. Two-point probe measurements confirmed the Ag wires to be disconnected as no conductance could be measured.

Water, as dispersing agent of the Ag–PAA NPs, was found to be not ideal to pattern Ag wires via MIMIC, as the evaporation was slow (1–2 h) and caused a drag of NPs out of the channel upon final evaporation. A more quickly evaporating, polar protic solvent that is suitable to pattern the Ag–PAA NPs with MIMIC was found to be methanol (MeOH).[17,18] The NP dispersion in MeOH was stable for about one day, with an average particle size of 28 $\pm$ 13 nm one hour after preparation (average particle size in water 21 $\pm$ 13 nm). The fast evaporation of MeOH and partial uptake by the PDMS mold within ~15 s allowed several passes of dispensing and complete evaporation to increase the amount of Ag–PAA NPs in the channels. Centimeter long Ag wires were thus obtained on PET (See Fig. S3, ESI†) with a line edge roughness of ~1.2 $\mu m$. An average layer thickness of ~1.5 $\mu m$ was obtained (See

Fig. S4, ESI†). Sintering was induced by 5 min exposure to HCl vapor at room temperature.

From a measured resistance of 4.66 Ω over a wire length of 449 μm with a cross-sectional area of $148 \pm 13$ μm$^2$, a resistivity of $326 \pm 110$ μΩcm (average over three wires) with a minimum of 154 μΩcm was calculated for MIMIC-patterned, sintered Ag microwires on PET foil from a Ag–PAA NP dispersion in MeOH. A very high resistivity of $1.3 \times 10^{10}$ μΩcm was measured before sintering. The evident transition in the resistivity before and after sintering shows clearly the effect of particle destabilization and sintering on the conductance of the wire. Before sintering, the packed Ag NPs are basically non-conducting. Sintering reduced the resistivity drastically, but it remained roughly a factor 8.5 higher than the value obtained from the aqueous dispersion. Two possible reasons could be the cause for such a relatively high resistivity. The first reason is related to particle packing: the chosen solvent, MeOH, did not stabilize the Ag–PAA NPs as good as water, leading to pre-coalescence and clustering in the dispersion. Most evidently, this was observed from the steady (but slow) separation of larger particle clusters from the ink dispersion. After about one day, most of the particles had precipitated. Additionally, the fast evaporation of MeOH might not provide sufficient time for optimal particle packing before complete solvent evaporation. The second reason for the observed high resistivity might be incomplete sintering. The cross-sectional area $A$ was calculated under the assumption, that all Ag–PAA NPs in the trench were destabilized and therefore sintered. However, the HCl vapor introduced to destabilize the Ag–PAA NPs to form conductive Ag microwires, might only induce sintering at the top surface of the ∼1.5 μm thick microwire. The lower part of the filled channel is then shielded from the HCl vapor, leading to a potentially thick non-sintered and strongly non-conductive part of the Ag wire. Thus, the calculated value for $A$ might not correspond to the sintered metallic cross section, consequently leading to an overestimated resistivity.

The proposed incomplete sintering was further investigated by the fabrication of thinner (∼$529 \pm 9$ nm; Fig. 3) Ag wires on PET. With a single run of MIMIC, the Ag–PAA NPs



Fig. 3 Atomic force microscopy image of a sintered, MIMIC-patterned Ag wire on PET foil, formed from Ag–PAA NPs dispersed in MeOH.

dispersed in MeOH did not form a connected wire. By two cycles of MIMIC and determination of their resistivity, an average resistivity of $1.2 \pm 0.3$ mΩcm with a minimum of 1 mΩcm was obtained, from a measured resistance of 41 Ω over a wire length of 216 μm with a cross-sectional area of 53 μm.

For the thinner Ag wires, formed from Ag–PAA NPs dispersed in MeOH, an even higher resistivity was obtained when compared to the thicker wires. At first instance, this does not support the proposed, limited sintering depth. However, the more inhomogeneous layer thickness and the large amount of grain boundaries makes a fair comparison difficult. From the results, no conclusive effect of the sintering depth can be determined for the NPs in MeOH, and further work would be beneficial to investigate this issue. In conclusion, fabrication of lines using MIMIC with aqueous solutions results in wires with the largest conductivity.

## Embedded Ag wires on PET foil

A method to fabricate metal structures embedded in SU8 is described in Scheme 1b. Hundred micron wide and spaced, 10 μm deep trenches were photolithographically patterned in a SU8 layer, after deposition on PET foil. The surface energy of SU8 was increased by a short O$_2$ plasma treatment, reducing the static contact angle of SU8 from $74.8 \pm 1.5°$ to <5°, to improve the wetting by the aqueous Ag–PAA NP solution. The Ag–PAA NP ink was placed at the entrance of the open microchannels by micropipetting (Scheme 1b1), whereafter the ink filled the open microchannels within 5 s under capillary forces (Scheme 1b2). After drying, the filling process was repeated to obtain a thicker layer. Sintering of the Ag–PAA NPs was induced to form Ag wires embedded in SU8 on PET (Scheme 1b3 and Fig. S5, ESI†).

From a measured resistance of 0.99 Ω over a wire length of 227 μm with a cross-sectional area of $237 \pm 14$ μm$^2$ (see Fig. S6, ESI†), an average resistivity of $128 \pm 22$ μΩcm with a minimum of 103 μΩcm was obtained using Ag–PAA NPs in water. The resistivity is much higher than the resistivity of 17.9 μΩcm obtained for MIMIC-patterned structures. As the aqueous dispersion is identical to the one used in MIMIC patterning, poorer packing is unlikely to be the reason for this high value. Again, the limited conductivity might be attributed to incomplete sintering of the 2.5 μm thick Ag microwire. In comparison to the previously MIMIC-patterned wire, only the top side of the embedded Ag–PAA NPs wires is exposed to HCl vapor, the other sides are covered (protected) by the chemically resistant SU8.

The proposed deficiency in sintering depth was further investigated by the fabrication of thinner (∼$953 \pm 14$ nm) Ag wires in the channel by one time filling, and determination of their resistivity. From a measured resistance of 0.84 Ω over a wire length of 464 μm with a cross-sectional area of 64 μm, an average resistivity of $14.9 \pm 3.7$ μΩcm (average over 5 wires) with a minimum of 11.6 μΩcm was obtained for Ag wires embedded in SU8 formed from an aqueous Ag–PAA NP dispersion. The much lower and excellent resistivity obtained for the thinner Ag wires embedded in the SU8 channels, only a factor ∼7 higher than bulk silver, clearly supports the validity of the earlier proposed incomplete sintering in the 2.5 μm thick Ag wires. Furthermore, the value for the resistivity of
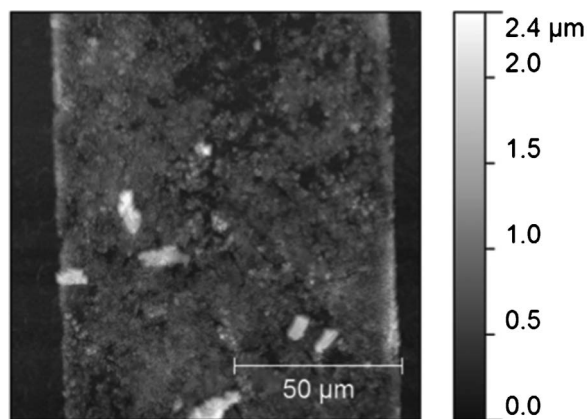
these thinner wires is in between the values for the prematurely self-sintering and non-optimally packing Ag NP dispersion with incorporated NaCl (16 $\pm$ 2.2 $\mu\Omega$cm[15]) and the extremely low resistivity (3.84 $\mu\Omega$cm[15]) reported for the 500 nm thick, HCl-sintered Ag–PAA NPs. Because the presence of a non-sintered region at the bottom of the 950 nm thick Ag layer cannot be excluded, the actual resistivity might be even lower than the value reported by us here.

To obtain a better insight in the actual sintering depth and the likeliness of a non-sintered core in the patterned Ag microwires leading to an overestimation in calculated cross-sectional area and therefore a higher resistivity, a sintered layer thickness was calculated under assumption of the best possible resistivity. The lowest reported resistivity for the aqueous Ag–PAA NPs is 3.84 $\mu\Omega$cm.[15] With measured quantities for the resistance, wire length and width, and the best reported resistivity, an ideally expected layer thickness could be calculated from equation 1. The calculated, fully sintered layers were surprisingly thin: A sintered layer thickness of 130 nm was calculated for the 604 nm thick, MIMIC-patterned Ag wire on PET. For the SU8-embedded Ag wires, conducting layer thicknesses of 88 nm and 212 nm were obtained for the 2.5 $\mu$m and 950 nm thick wires, respectively. While the first two values indicate a maximal sintering depth of around 100 nm, the thinner Ag microwire embedded in SU8 seems to be sintered twice as deep. It can also be interpreted as an indication for a sintering depth of $\sim$100 nm in combination with an improved particle packing. Therefore, particle packing could be better in case the wires were fabricated in open microchannels compared to wires patterned with MIMIC. The calculated sintering depths of Ag wires, formed from Ag–PAA NPs dispersed in MeOH, are much less. Sintering depths of only 37 nm and 20 nm were calculated for the 1.5 $\mu$m and 529 nm thick wires, respectively. The calculated, very low sintering depths obtained from wires fabricated from Ag–PAA NPs dispersed in MeOH are clearly different from structures made from the aqueous dispersion. It strongly suggests a disadvantageous particle packing and possible size distribution as a result of the rather instable MeOH dispersion.

The overestimation in resistivity as a result of a non-sintered core in the thick Ag wires was studied by applying Ag–PAA NP ink repeatedly in SU8 matrices as described in Scheme 1b. In the first sample, the channels were filled with Ag–PAA NP ink and dried. This process was repeated two times. After the threefold filling, the complete structure was sintered by exposure to HCl vapor, potentially resulting in a non-sintered core in the wires. In the second sample, the channel was filled with ink, dried and directly sintered. This process was repeated two more times. Thus, this resulted in three sintered layers deposited on top of each other to constitute the wires. Again, we calculated the sintering depth under the assumption of the best possible resistivity of 3.84 $\mu\Omega$cm,[15] resulting in a nearly 9 times higher sintering depth of the in-between sintered Ag wires compared to the three times filled and sintered-once Ag wires.

The result of this experiment indicate even more strongly the presence of a non-sintered core in the thick Ag wires. More study is required to investigate the sintering process and depth itself, as a function of the sintering medium and wire geometry. For now, it can be concluded that most optimally sintered wires were obtained using thin particle layers, deposited from aqueous solution, followed by sintering, and that thicker metal structures should be made by growing and sintering the structures in a stepwise manner.

### Sol–gel printed Ag dots on an elastomeric surface

To study an alternative patterning technique with the potential for printing metal dots with a resolution not typically obtained by inkjet printing, Ag–PAA NPs in water were printed from hydrogel reservoirs in a stamping device to form arrays of Ag dots with a diameter of only a few microns.

Reservoirs were fabricated in Si by photolithography and standard KOH etching techniques. A master containing 25 reservoirs each with 144 pores of 5 $\mu$m width and a 25 $\mu$m membrane, according to a procedure reported earlier by our group,[19,20] was fabricated. A hydrogel was formed in the reservoirs, constituting an intertwined network with submicron porosity. The hydrogel facilitates ink uptake and transfer similar to a stamping pad. After inking the hydrogel for 2 h with a Ag-PAA NP solution, the stamping device was pressed against a freshly activated, unpatterned slab of PDMS.

Up to eight sequential prints on different areas of the substrate with a total volume of 50 $\mu$L Ag–PAA NPs were performed, printing arrays of 144 Ag dots each (Fig. 4).

The SEM images in Fig. 4a–c display, with increasing magnification, one array of printed Ag dots on PDMS. Only one defect can be seen from the overview image in Fig. 4a. The higher magnification in Fig. 4b displays the irregular shape of the dots before sintering, and from the highest magnification image in Fig. 4c a dot diameter of $\sim$4.6 $\mu$m can be inferred. From the AFM image of a different, smaller printed dot in Fig. 4d, an average height distribution of 98 nm and a root mean square (rms) roughness of 27 nm can be extracted. The height profile in Fig. 4e shows a dot width of around 2 $\mu$m and gives an impression of the overall height distribution and roughness of a printed Ag dot.

Further analysis of the feature height and overall surface roughness was performed by measuring twenty individual, sintered Ag dots of a printed array with AFM (one dot shown in Fig. 4f). An average height of 266 nm with a relatively small standard deviation of $\sim$12% over 20 printed dots was obtained. From the maximal height difference of 474 nm from the highest (average maximum height 579 $\pm$ 108 nm) to the lowest point per dot (average minimal height 105 $\pm$ 24 nm), a non-flat top side can be concluded. From the average projected area over all 20 dots (6.8 $\pm$ 1.0 $\mu$m), and under the assumption of a circular shape, an average diameter of 3 $\mu$m was calculated.

SEM imaging (data not shown) of all eight sequential prints on PDMS showed a decrease in feature size and an increasing number of defectively printed dots per array (up to 17 defects over 144 dots in one array). Counted as defectively printed were all missing or very small (<1.2 $\mu$m) Ag dots. For every print, the width of 20 dots was measured from the SEM images and averaged, showing a steady decrease from 5.7 $\pm$ 1.3 $\mu$m to 3.5 $\pm$ 0.6 $\mu$m. The increase in defects and decrease of the printed dot size can originate from two factors: ink depletion
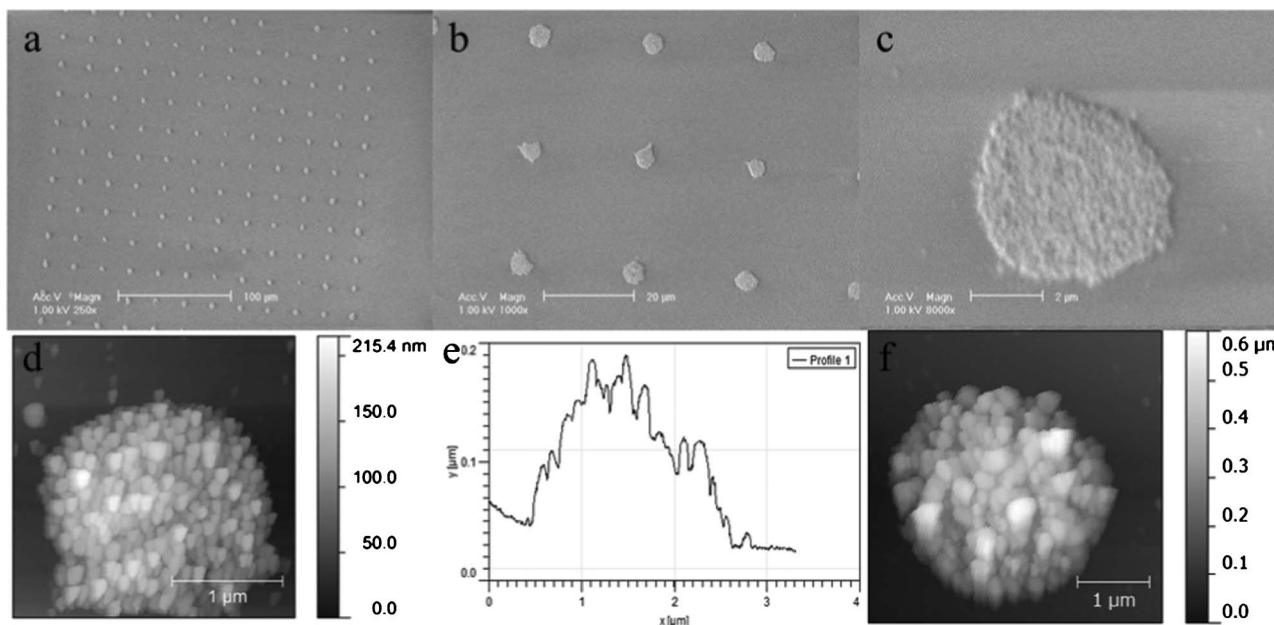
**Fig. 4** Scanning electron (a–c) and atomic force microscopy images and profile (d–f) of hydrogel-printed, non-sintered (a–e) and sintered (f) Ag–PAA dots on PDMS. (a) Array of 144 Ag dots with close-ups shown in (b) and (c). (d) AFM height image and (e) corresponding profile of an individual Ag dot. (f) AFM height image of a sintered Ag dot.

and clogging. During printing, the hydrogel turned slowly silvery grey; an indication for sintering of the Ag–PAA NPs while still present in the hydrogel. Furthermore, no increase in feature size was observed after re-inking the hydrogel after the fourth print, which would be expected if ink depletion were the cause. Therefore, clogging of the fine pores caused by particle sintering is the most likely cause for the decreasing printing quality.

These results demonstrate the utilization of the hydrogel stamping device to print Ag dots from a Ag NP dispersion at a few-micron scale. The hydrogel allows to combine the qualities of spotting with the high resolution of microcontact printing. On average, Ag dots of $5.7 \pm 1.3$ μm have been printed on PDMS in eight sequential prints, with re-inking after the fourth print. With a continuous printing technique, or a denser array, Ag droplets might be able to merge before solvent evaporation and form conductive lines or features, offering an innovative extension to the patterning of room temperature-sintering particles.

## Experimental section

### Ag NP synthesis

Silver nanoparticles were synthesized by the reduction of silver acetate with ascorbic acid in the presence of poly(acrylic acid) sodium salt ($M_w = 8000$), similar to the procedure reported by Magdassi et al.[9] In short, 2.25 g silver acetate (Acros) and 0.934 g 45 wt% poly(acrylic acid) sodium salt ($M_w = 8000$, Aldrich) were mixed and heated to 95 °C for 15 min in 14 mL of MilliQ water. Then, 1.7 g 30 wt% L-ascorbic acid (Aldrich) was slowly added, and the mixture was stirred for 30 min while heating.

The obtained nanoparticles were washed by centrifugation, and the obtained sediment was redispersed in MilliQ water. The pH of the dispersion was adjusted to 9.5 by the addition of 2-amino-2-methyl-1-propanol 95% (Aldrich). Directly before use, the dispersion was sonicated for 5 min. The Ag–PAA NPs were found to be very stable in water. The particle size was determined by dynamic light scattering to be $21 \pm 13$ nm (number average over five measurements) after half a year storage in a fridge. The Ag–PAA NP dispersion in MeOH was prepared by evaporating the water from 200 μL of the aqueous dispersion at 60 °C in an oven. The dried particles were redispersed in 200 μL MeOH and sonicated for 5 min. After sedimentation of a few secondary particles, the supernatant was used as the ink.

### Ag NP sintering

Room temperature sintering of the patterned Ag–PAA NPs was induced by exposing the sample for 5 min at a distance of $\sim 2$ cm to a 37% HCl solution.

### Preparation of PDMS molds

The mold material, Sylgard-184 poly(dimethyl siloxane) (PDMS), was purchased from Dow Corning. PDMS molds were prepared by mixing the curing agent and the prepolymer manually in 1 : 10 volume ratio and curing overnight at 60 °C against a photolithographically patterned Si master. After curing, the PDMS molds were peeled off from the Si wafer.

### Preparation of SU8 trenches on PET

Trenches in SU8-5 of 100 μm width and 9 μm depth were fabricated by standard photolithographic patterning on 200 μm thick PET foil (Kodak). For achieving an improved

adhesion, PET was exposed to $O_2$ plasma (18 sccm) for 1 min using a Tepla 300 UCL at 300 W. SU8-5 (MicroChem) was deposited on the activated PET foil by spincoating for 10 s at 500 rpm and 30 s at 1500 rpm, followed by a soft bake program starting at 25 °C, holding the temperature at 50 °C for 1 min, at 65 °C for 1 min, and at 95 °C for an additional 3 min after which the temperature was slowly decreased to 25 °C. With a mask aligner (EVG620), the SU8 was exposed for 13 s at a proximity of 20 μm. A post-exposure bake starting at 25 °C, holding the temperature at 50 °C for 1 min, at 65 °C for 1 min, and at 80 °C for an additional 2 min after which the temperature was slowly decreased to 25 °C, was followed by 90 s development in RER600, rinsing with isopropanol and blow drying by $N_2$.

### Hydrogel stamps

A Si stamping device with hydrogel reservoirs was fabricated according to literature.[20] In short, a chip with 25 reservoirs, each holding 144 pores of 5 μm width and a 25 μm membrane, was fabricated with standard photolithographic patterning and KOH etching of a silicon-on-insulator (SOI) wafer. The chips were cleaned in Piranha solution (3 : 1 mixture of conc. sulfuric acid and 30% hydrogen peroxide. CAUTION! Piranha solutions should be handled with great care in open containers in a fume hood. Piranha is highly corrosive, toxic and potentially explosive) for 30 min and subsequently rinsed with MilliQ water, ethanol and then blown dry with $N_2$. The chip was functionalized with 1*H*,1*H*,2*H*,2*H*-perfluorodecyltrichlorosilane (PFDTS) (ABCR) overnight. By exposure to $O_2$ plasma, PFDTS was removed from the chip except for the printing side of the chip. The inner walls of the reservoir were functionalized and the pores filled with a hydrogel.[20] As initiator, ammoniumpersulfate and tetramethylethylenediamine were added under Ar atmosphere. The hydrogel-filled reservoirs were kept under water until use.

To print with the hydrogel reservoirs, 5–10 μL AgPAA NPs dispersion was micro-pipetted on the reservoirs and left for ∼2 h, allowing the ink to penetrate the hydrogel. Just before printing, excess ink was removed and the loaded chip was gently pressed against UV/O3-activated PDMS. After a few seconds, the chip was gently removed.

## Conclusions

In summary, silver wires were patterned on PET foil by MIMIC, and silver wires embedded in SU8 were fabricated on PET foil by wetting-controlled deposition in open microchannels. One hundred μm-wide Ag microwires with a length of 5–15 mm and a height of 0.6–2.5 μm were fabricated. The influence of the solvent on the resistivity was studied by replacing water for MeOH in the Ag–PAA NP dispersion. The MIMIC process was sped up with MeOH as the solvent and the layer thickness could be increased by multiple cycles of MIMIC. However, the MeOH based Ag–PAA NP dispersion was only semi-stable for a maximum of one day and resulted in higher measured resistivities as a result of disadvantageous particle packing and pre-coalescence of the NPs in solution. Sintering was in

most cases performed with HCl vapor. Wires patterned with the self-sintering aqueous Ag–PAA NP dispersion with added NaCl in a concentration below 50 mM, did not result in a continuous pattern. As a result, only interrupted and non-conducting Ag wires could be fabricated on PET foil with this self-sintering ink. Furthermore, a layer thickness dependence was found for the wire resistance. Thicker wires showed a higher resistivity than thinner wires. This is attributed to incomplete sintering of the Ag wires, due to a blocked penetration of the HCl vapor into the bulk material after sintering of the top layer. As a result, the calculated values for the cross-sectional area $A$ in equation 1 were typically overestimated, leading to calculated resistivities higher than those most likely occurring in the well-sintered top layer. Additionally, particle packing in the channel might be less optimal with MIMIC, due to contact angle-dependent drag of the contact line to the channel sidewalls.

With Ag–PAA NP-loaded hydrogel reservoirs, arrays of 144 Ag dots each have been repetitively printed on PDMS in eight sequential prints. From a statistical study over 20 sintered dots, average diameter and height were determined to be approx. 3 μm and 266 nm, respectively. The submicron porosity of the hydrogel allowed a critical control over ink uptake and release. A growing number of defects was found, in the sense of non-printed or very small dots, upon increased print number. Up to 17 defects, out of 144 dots, were counted for the eighth print.

The here utilized, room temperature-sintering Ag–PAA NPs show an enormous potential and compatibility for use in flexible electronics. Other Ag NP formulations generally require high annealing temperatures up to 320 °C for up to 30 min,[14] to obtain conductivities in the here reported range, although efforts are made to reduce this temperature also for other formulations. Although we did not obtain the 41% conductivity reported by Grouchko *et al.*,[15] a factor 7.3 lower conductivity than bulk Ag is a very good result. The resistivity might be even decreased further, by reduction of the layer thickness or by ensuring full layer sintering by other particle destabilizing reactions. In the case of hydrogel printing, using hydrogels with a larger porosity and the use of cleaning procedures may even increase the number of possible printing steps. Such dot patterns may be useful in (*e.g.* Raman) sensing and optical devices.

## Acknowledgements

## References

1 J. Perelaer, P. J. Smith, D. Mager, D. Soltman, S. K. Volkman, V. Subramanian, J. G. Korvink and U. S. Schubert, *J. Mater. Chem.*, 2010, **20**, 8446–8453.

2  A. Sazonov, D. Striakhilev, C. H. Lee and A. Nathan, *Proc. IEEE*, 2005, **93**, 1420–1428.

3  T. Kietzke, *Adv. Opt. Electron.*, 2007, 40285.

4  F. C. Krebs, H. Spanggard, T. Kjær, M. Biancardo and J. Alstrup, *Mater. Sci. Eng., B*, 2007, **138**, 106–111.

5  H. Sirringhaus, T. Kawase, R. H. Friend, T. Shimoda, M. Inbasekaran, W. Wu and E. P. Woo, *Science*, 2000, **290**, 2123–2126.

6  P. F. Baude, D. A. Ender, M. A. Haase, T. W. Kelley, D. V. Muyres and S. D. Theiss, *Appl. Phys. Lett.*, 2003, **82**, 3964–3966.

7  A. Russo, B. Y. Ahn, J. J. Adams, E. B. Duoss, J. T. Bernhard and J. A. Lewis, *Adv. Mater.*, 2011, **23**, 3426–3430.

8  V. Subramanian, J. M. J. Frechet, P. C. Chang, D. C. Huang, J. B. Lee, S. E. Molesa, A. R. Murphy, D. R. Redinger and S. K. Volkman, *Proc. IEEE*, 2005, **93**, 1330–1338.

9  S. Magdassi, M. Grouchko, O. Berezin and A. Kamyshny, *ACS Nano*, 2010, **4**, 1943–1948.

10  Z. Zhang, X. Zhang, Z. Xin, M. Deng, Y. Wen and Y. Song, *Nanotechnology*, 2011, **22**, 425601.

11  S. B. Walker and J. A. Lewis, *J. Am. Chem. Soc.*, 2012, **134**, 1419–1421.

12  S. Gamerith, A. Klug, H. Scheiber, U. Scherf, E. Moderegger and E. J. W. List, *Adv. Funct. Mater.*, 2007, **17**, 3111–3118.

13  P. Smith, D. Y. Shin, J. Stringer, B. Derby and N. Reis, *J. Mater. Sci.*, 2006, **41**, 4153–4158.

14  B. J. Perelaer, A. W. M. de Laat, C. E. Hendriks and U. S. Schubert, *J. Mater. Chem.*, 2008, **18**, 3209–3215.

15  M. Grouchko, A. Kamyshny, C. F. Mihailescu, D. F. Anghel and S. Magdassi, *ACS Nano*, 2011, **5**, 3354–3359.

16  J. Perelaer, R. Jani, M. Grouchko, A. Kamyshny, S. Magdassi and U. S. Schubert, *Adv. Mater.*, 2012, **24**, 3993–3998.

17  W. M. Haynes, CRC Press/Taylor and Francis, Boca Raton, FL.

18  C. M. Hansen, *Hansen solubility parameters: a user's handbook*, CRC Press/Taylor and Francis, Boca Raton, Fl., 2007.

19  E. Bat, P. Jonkheijm, A. van Amerongen and J. Huskens, *EP12186681.8*, 2013.

20  E. Bat, J. Cabanas Danés, P. F. Moonen, G. H. Posthuma-Trumpie, A. Van Amerongen, J. Huskens and P. Jonkheijm, *in preparation*, 2013.